PROCEEDINGS OF SCIENCE

Using Coupled-Channel Approaches to Explore Photoproduced $\eta^{(\prime)}\pi^0$ Systems in the Search for Exotic Hadrons at GlueX

Zachary Baldwin[a,*] **for the GlueX Collaboration**

[a] *Carnegie Mellon University,*
Pittsburgh PA, United States of America

E-mail: zbaldwin@cmu.edu

Probing the non-perturbative regime of Quantum Chromodynamics (QCD) remains a critical challenge in hadron spectroscopy, particularly concerning the role of gluonic excitations in determining the hadronic spectrum. The GlueX experiment at Jefferson Lab is designed to address this challenge through the search for exotic hybrid mesons, states predicted by QCD to include gluonic degrees of freedom beyond the conventional quark-antiquark framework. This presentation highlights the ongoing amplitude analyses of the $\eta\pi$ and $\eta'\pi$ systems, produced via photoproduction with a polarized photon beam. Recent efforts involve refining resonance modeling through the usage of mass-dependent parameterizations that embed proper physics constraints. These developments aim to enhance the robustness of amplitude fits and improve their sensitivity to potential underlying exotic contributions. The resulting analyses offer a clearer window into hadronic structure and provide a step forward in the experimental exploration of QCD's predicted exotic hadrons.

The European Physical Society Conference on High Energy Physics (EPS-HEP 2025)
6-11 July, 2025
Palais Du Pharo, Marseille, France

*Speaker

PoS(EPS-HEP2025)255

1. Introduction

The light-quark meson spectrum allows for a sensitive test of non-perturbative Quantum Chromodynamics (QCD) and of how gluonic degrees of freedom enter hadron structure. In particular, hybrid mesons are states in which the gluon field is excited in addition to the underlying quark-antiquark pair. They are a generic consequence of QCD and can carry quantum numbers that are forbidden to conventional $q\bar{q}$ states. Lattice QCD calculations in the light-quark sector [1] and QCD inspired phenomenological models [2, 3] predict light hybrid mesons including states with exotic quantum numbers $J^{PC} = 1^{-+}$ in the light-quark sector. Conventionally, the isovector state is commonly denoted as the π_1.

Experimentally, the situation is unsettled. Signals with 1^{-+} quantum numbers have been reported in $\eta\pi$ and $\eta'\pi$ with different masses and widths, and are commonly labeled the $\pi_1(1400)$ and the $\pi_1(1600)$. COMPASS specifically has observed an enhancement near 1.4 GeV in $\eta\pi$ and a peak around 1.6 GeV in $\eta'\pi$, which in traditional single-channel analyses are often interpreted as evidence for two distinct exotic resonances below 2 GeV [4]. However, such a two-state interpretation is already problematic from the point of view of spectroscopy and decay patterns, since it would require two 1^{-+} isovector states separated by only about 200 MeV, with one decaying almost exclusively to $\eta\pi$ and the other predominantly to $\eta'\pi$ while essentially not coupling to $\eta\pi$. This illustrates how isolated Breit-Wigner fits applied to a dense spectrum with overlapping structures and multiple coupled decay channels can produce apparent structures that depend strongly on the chosen parameterization, thereby motivating a coupled-channel framework for a consistent description.

A recent JPAC coupled-channel analysis of COMPASS $\pi p \to \eta^{(\prime)}\pi p$ data demonstrated that a single exotic π_1 pole, with nonzero residues in both $\eta\pi$ and $\eta'\pi$, already suffices to describe the observed P-wave enhancements, while simultaneously accounting for the $a_2(1320)$ and $a_2'(1700)$ in the D wave [5]. The goal of this work is to assess how this coupled-channel scenario carries over to GlueX photoproduction of $\eta\pi^0$ and $\eta'\pi^0$ by establishing a validated analysis implementation and performing closure tests on pseudo-data to help determine whether a common coupled-channel description can accommodate both hadroproduction and photoproduction with the same lightest π_1 pole.

1.1 The GlueX experiment

Located in Hall D at the Thomas Jefferson National Accelerator Facility (Jefferson Lab) is the *Glu*onic *Ex*citation experiment (GlueX). An electron beam of up to 12 GeV impinges on a thin diamond radiator to produce a bremsstrahlung photon beam that is energy tagged by a dedicated magnetic spectrometer. The bremsstrahlung is produced by the diamond radiator and exhibits a coherent enhancement, yielding a linearly polarized photon spectrum with a well defined coherent peak, which is essential for detailed studies of the hadron production mechanism in exclusive photoproduction in amplitude analyses. The tagged photon beam is directed onto a liquid hydrogen target surrounded by a nearly hermetic detector. This detector configuration provides large geometrical acceptance and good resolution for both charged tracks and photons in the kinematic region relevant for the exclusive reactions enabling the coupled-channel studies presented in this work [6].

The experiment was explicitly designed to reconstruct exclusive reactions such as $\gamma p \to pM$ with M decaying into multihadron final states, including channels with several neutral mesons, and has already collected a large data set with linearly polarized photons. In Phase I, GlueX has accumulated an integrated luminosity of roughly 125 pb^{-1} in the coherent peak region of the photon spectrum, with Phase II ongoing and projected to deliver about three to four times more integrated luminosity. The combination of high precision data sets, controllable photon polarization, and nearly uniform acceptance for $\eta^{(\prime)}\pi$ topologies makes GlueX uniquely suited to study photoproduction of candidate hybrid mesons and to test coupled-channel parameterizations originally developed for hadroproduction, providing direct sensitivity to the π_1 pole and its channel-dependent residues.

2. Coupled-Channel Framework

Amplitude analyses in the light-meson sector have traditionally relied on models based on sums of Breit-Wigner terms fitted independently in each decay channel. That approach is best controlled when states are narrow, well separated, and when there is no significant inelasticity. In the $\eta^{(\prime)}\pi$ system none of these assumptions hold as several states with the same quantum numbers overlap, important additional decay channels open in the relevant mass region, and the associated branch points constrain the analytic structure. For such a situation, a naive sum of Breit-Wigners generically violates unitarity and analyticity, and the fitted masses and widths may become strongly model-dependent, rather than being fundamental properties of the underlying S-matrix. Modern analyses therefore adopt explicitly unitary coupled-channel frameworks, such as K-matrix parameterizations with P-vectors, dispersive N/D constructions, or related approaches that build the correct analytic structure into the amplitude from the outset.

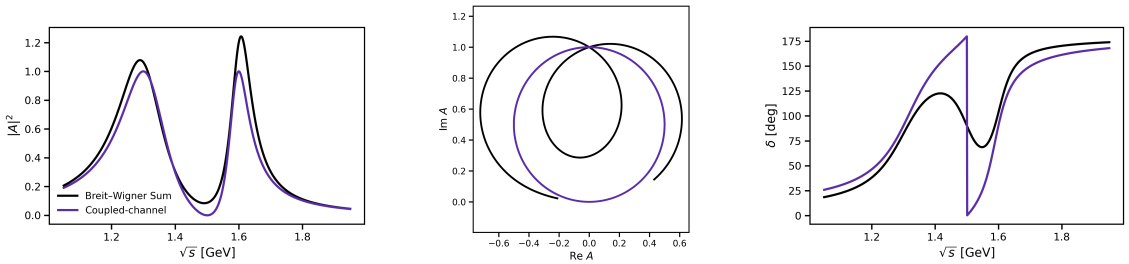

(a) **(b)** **(c)**

Figure 1: Comparison of a unitary coupled-channel amplitude (purple) with a sum of isolated Breit-Wigner terms fitted in a single channel (black) for a toy model with two nearby resonances. Panel (a) shows the intensity reproduced by both models, panel (b) shows the Argand trajectory, and panel (c) shows the phase motion. Although both models reproduce the peak structures in the intensity, the Breit-Wigner sum model misdescribes the interference, does not remain on or within the unitarity circle in the Argand representation, and produces an unphysical non-monotonic behavior in the phase motion.

This point is illustrated in Fig. 1, which compares a toy model constructed from a sum of two Breit-Wigner amplitudes to a unitary coupled-channel-inspired parameterization with the same pole content. In panel (a) both descriptions have been tuned to reproduce nearly identical peak structures in the intensity $|A|^2$, so line shapes alone do not diagnose the problem. The differences become evident in the phase motion and Argand trajectory. In panel (b), the unitary amplitude traces a single, well-behaved loop in the complex plane, as expected for a unitary amplitude, while the Breit-Wigner model produces a multi-loop Argand curve characteristic of interfering, non-unitary contributions, which demonstrates why a coupled-channel framework is essential for the present analysis. In panel (c), the unitary amplitude exhibits a smooth, monotonic phase evolution governed by the poles, whereas the Breit-Wigner sum develops a distorted phase with an unphysical kink between the peaks.

2.1 JPAC model description

In the JPAC analysis of $\eta^{(\prime)}\pi$ [5] the partial-wave production amplitudes $a_i^J(s)$ are written in an N/D representation that cleanly separates the known kinematic factors from a smooth production term and a coupled-channel denominator whose dispersive construction encodes the two-body $\eta^{(\prime)}\pi$ interaction. This model was developed to describe the diffractive reaction $\pi p \to \eta^{(\prime)}\pi p$ measured by COMPASS at high energy, where production is dominated by Pomeron exchange and factorizes into a $\pi\mathbb{P} \to \eta^{(\prime)}\pi$ subprocess that can be treated at fixed momentum transfer [5].

For a given angular momentum J and channel index i, the amplitude is

$$a_i^J(s) = q^{J-1}(s)\, p_i^J(s) \sum_k n_k^J(s) \left[D^J(s)^{-1}\right]_{ki}, \tag{1}$$

where q denotes the magnitude of the incoming pion momentum in the $\eta^{(\prime)}\pi$ center-of-mass frame, p_i is the breakup momentum in channel i. The prefactor $q^{J-1}p_i^J$ takes into account angular-momentum barriers. Following Ref. [5], one unit of incoming momentum is divided out to account for the Pomeron-nucleon vertex in the diffractive production mechanism. The real-valued, slowly varying functions $n_k^J(s)$ parametrize the production mechanism into channel k, while all non-trivial analytic structure associated with two-body $\eta^{(\prime)}\pi$ scattering is collected in the common denominator matrix $D^J(s)$.

The matrix $D^J(s)$ is constructed from a dispersion relation. On the real axis it can be written schematically as

$$D_{ki}^J(s) = \left[K^J(s)^{-1}\right]_{ki} - \frac{s}{\pi}\int_{s_k}^{\infty} \frac{ds'}{s'(s'-s-i\epsilon)}\, \rho N_{ki}^J(s'), \tag{2}$$

where $K^J(s)$ is a real-valued K-matrix and s_k denotes the threshold of channel k. The function $\rho N_{ki}^J(s')$ provides an effective description of left-hand singularities in $\eta^{(\prime)}\pi \to \eta^{(\prime)}\pi$ scattering and enters as the integrand of the dispersive integral that generates the right-hand cut in $D^J(s)$. The K-matrix is parameterized as a sum of bare poles plus a smooth background,

$$K_{ki}^J(s) = \sum_R \frac{g_k^{J,R} g_i^{J,R}}{m_R^2 - s} + c_{ki}^J + d_{ki}^J\, s, \tag{3}$$

with real-valued couplings $g_i^{J,R}$ and real symmetric matrices c_{ki}^J and d_{ki}^J in the channel indices. In their reference model, the D-wave contains two 2^{++} poles, associated with the $a_2(1320)$ and $a_2'(1700)$, while the exotic P-wave contains a single 1^{-+} pole [5].

We use the JPAC model in this work to describe the $\eta^{(\prime)}\pi$ two-body subsystem dynamics in $\gamma p \to p\eta^{(\prime)}\pi^0$ and keep all parameters of the coupled-channel scattering amplitude fixed to the hadroproduction fit. The JPAC parametrization was developed for diffractive pion dissociation with a pion beam and therefore contains production specific conventions appropriate to that reaction, which we retain unchanged in this zeroth-order photoproduction implementation. Extensions of the production model required for a photoproduction setting are currently being developed. At this stage, photoproduction effects are introduced only through overall complex photocouplings multiplying each partial wave and channel. In the current Monte Carlo studies and in future fits to GlueX data, this strategy ensures that GlueX constrains the relative production strengths and phases, while the fixed pole content and coupled-channel line shapes encoded in $D^J(s)$ are taken directly from the COMPASS analysis.

2.2 Line shapes

As a validation step, we compute the $\eta^{(\prime)}\pi$ P- and D-wave line shapes from the coupled-channel N/D amplitudes of Ref. [5], using the published parameter values and the dispersive representation of Sec. 2.1. For each channel $i = \eta\pi, \eta'\pi$ we evaluate the complex partial-wave amplitudes of Eq. (1) at $J = 1$ and $J = 2$ and denote $A_P^i(s) \equiv a_i^{J=1}(s)$ and $A_D^i(s) \equiv a_i^{J=2}(s)$. From these we form the intensities $I_{P,D}^i(s) = |A_{P,D}^i(s)|^2$ and the relative P-D phases, with the phase unwrapped into $[0, 360^\circ)$. In the numerical implementation, we restrict to $0.8 < m(\eta^{(\prime)}\pi) < 2.0$ GeV, matching the mass range used in the JPAC fit and shown in Fig. 1 of Ref. [5].

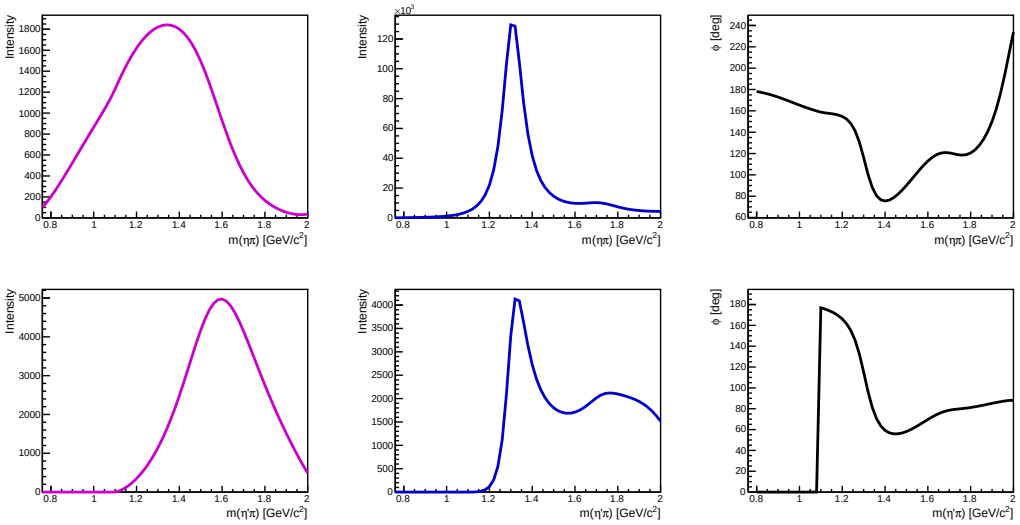

Figure 2: Computed JPAC $\eta^{(\prime)}\pi$ P- and D-wave intensities and P-D phase differences from the coupled-channel N/D amplitudes of Ref. [5]. The line shapes reproduce the published JPAC curves of Ref. [5], validating the implementation used in this work.

The resulting line shapes and phase differences shown in Fig. 2 demonstrate that our implementation reproduces the characteristic features of Ref. [5]. The broad exotic P-wave enhancements in $\eta\pi$ and $\eta'\pi$ are recovered. The $a_2(1320)$ and the $a_2'(1700)$ structures in the D-wave are also reproduced, together with the characteristic P-D phase motion. This level of agreement indicates that the numerical implementation and conventions reproduce the reference JPAC behavior.

3. Coupled-channel fits to Monte Carlo data

Before confronting the coupled-channel model with data, we choose a representative parameter set for the coupled-channel N/D amplitudes and use it to generate pseudo-data in a photoproduction environment using simulated signal Monte Carlo events for the reactions $\gamma p \to p\eta^{(\prime)}\pi^0$. Events are generated with the standard GlueX machinery, which incorporates the measured photon-energy spectrum and realistic distributions of the squared four-momentum transfer. For the studies shown here, we impose unit acceptance and omit the detector geometry and response, so that the resulting samples correspond to perfect acceptance. The event generation fixes the photoproduction kinematics, while the $\eta^{(\prime)}\pi^0$ mass dependence and partial-wave content are generated from the coupled-channel N/D amplitudes at the fixed reference parameter set. Accordingly, the resonance structures present in the pseudo-data arise from the chosen N/D solution itself, with no additional ad hoc line shapes or explicit spin-exotic contributions introduced at the generator level beyond those already encoded in the amplitude model.

The pseudo-data are then refit with the identical coupled-channel N/D parameterization, so that the study constitutes an input-output (closure) test of the implementation under GlueX-like kinematic conditions. Closure is assessed by comparing the refitted parameter values and derived partial-wave intensities to the generating reference values used to construct the pseudo-data. Normalization integrals are evaluated using large, statistically independent phase-space samples. With unit acceptance, these samples implement trivial acceptance corrections while preserving the standard normalization procedure used in the full analysis chain.

For each event we evaluate the partial-wave amplitudes $A_i^J(s)$ according to Eq. (1). The denominator matrices $D^J(s)$ and the Chebyshev-polynomial parameters that define $n_k^J(s)$ are fixed to the JPAC fit of the COMPASS $\eta^{(\prime)}\pi$ analysis. The only free parameters associated with these amplitudes are overall complex photocouplings multiplying each partial wave and channel. In

this approach, the coupled-channel $\eta^{(\prime)}\pi$ two-body amplitude constrained in hadroproduction is reused without modification in the photoproduction environment, while the refit determines only the relative production strengths and phases.

As demonstrated in Sec. 2.1, the numerical implementation reproduces the published Rodas et al. line shapes on the real axis. The coupled-channel $\eta^{(\prime)}\pi$ two-body amplitude model is taken to be common across production processes in the sense that its analytic structure (the fixed N/D denominator and numerator parameters) is held fixed, while the production mechanism enters only through overall complex couplings for each wave and channel. This setup is convenient for closure studies because it tests the numerical stability of the fixed coupled-channel N/D amplitude while leaving only overall complex wave-by-wave production couplings to be determined in the refit.

From this baseline implementation we retain the kinematic prefactor $q^{J-1}p_i^J$ from the hadroproduction analysis. In the GlueX application this prefactor plays the role of an effective natural-parity (Pomeron-like) exchange factor. Any mismatch between this approximation and the true photoproduction kinematics would primarily affect the extracted production couplings. The pole content of the fixed JPAC denominator $D^J(s)$ would be unchanged by construction.

Within this study, we use these pseudo-data closure tests to quantify the sensitivity of the GlueX topology to the coupled-channel P- and D-wave patterns and to verify that the fixed pole content can be carried through a photoproduction environment without numerical distortions of the line shapes. These studies demonstrate that the prominent D-wave structures associated with the $a_2(1320)$ and $a_2'(1700)$ remain clearly visible in $\eta\pi^0$ and $\eta'\pi^0$ over the full fitted mass range, and that the refits retain sensitivity to a strongly suppressed P-wave component in $\eta\pi^0$.

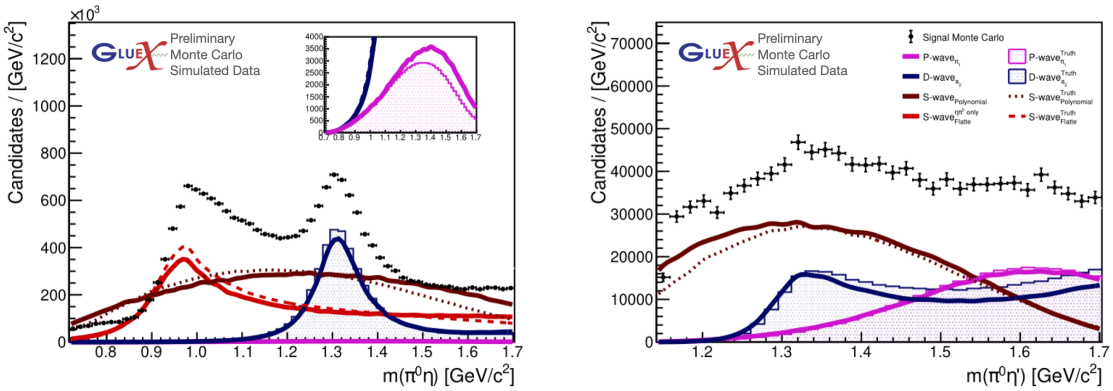

Figure 3: Reconstructed $\eta\pi^0$ (left) and $\eta'\pi^0$ (right) invariant-mass spectra from GlueX Monte Carlo pseudo-data (black points), overlaid with coupled-channel fits using fixed JPAC N/D amplitudes and free complex photocouplings. Solid curves show the fitted exotic P-wave (magenta), D-wave (blue), and S-wave components (light/dark red). The S-wave includes a Flatté term only in $\eta\pi^0$ and channel-dependent polynomial terms of the same functional form in both $\eta\pi^0$ and $\eta'\pi^0$. Hatched filled areas indicate the generated *truth* contributions for the P- and D-waves, while dashed/dotted red curves show the S-wave truth components. The inset enlarges the suppressed $\eta\pi^0$ P-wave contribution.

Figure 3 shows the resulting closure test. While the overall yield is dominated by S-wave contributions, the D-wave retains prominent resonant structure, including the characteristic $a_2(1320)$ peak along with the $a_2'(1700)$, whereas the exotic P-wave is strongly suppressed in $\eta\pi^0$ and substantially larger in $\eta'\pi^0$, reflecting the channel hierarchy encoded in the chosen coupled-channel solution. This qualitative hierarchy is consistent with the GlueX upper limits on $\pi_1(1600)$ photoproduction which imply that any $\pi_1(1600)$ contribution would be below the percent level in $\eta\pi$ while still allowing it to be a leading contribution in $\eta'\pi$, when interpreted with the branching fraction assumptions used in Ref. [7]. The same pattern is supported by lattice QCD results that find the lightest 1^{-+} hybrid to couple much more weakly to $\eta\pi$ than to $\eta'\pi$ [8].

4. Conclusions

The $\eta^{(\prime)}\pi$ systems remain a key testing ground for spin-exotic light-quark spectroscopy and for coupled-channel methods in a strongly inelastic regime. We implemented the JPAC coupled-channel N/D model for $\eta^{(\prime)}\pi$ in a form suitable for GlueX photoproduction, benchmarked the numerical implementation against the published COMPASS-based JPAC solution, and performed input-output (closure) tests using pseudo-data generated from a fixed representative parameter set. These closure refits demonstrate numerical self-consistency of the coupled-channel implementation in a GlueX-motivated kinematic environment.

In the exotic P-wave, the closure tests reproduce the strong channel hierarchy encoded in the generating coupled-channel solution, with a strongly suppressed $\eta\pi^0$ contribution and a much larger $\eta'\pi^0$ intensity in the a_2 region. The resulting P-wave hierarchy aligns qualitatively with external results, including the GlueX $\pi_1(1600)$ upper-limit study and lattice-QCD expectations for suppressed $\eta\pi$ relative to $\eta'\pi$ couplings [7, 8]. Overall, these results show that the coupled-channel dispersive framework can be deployed at the numerical level in a photoproduction setting. These closure and benchmarking studies support the use of coupled-channel dispersive parameterizations in this sector and highlight the limitations of purely single-channel Breit-Wigner descriptions in a strongly inelastic regime. Within the JPAC single-pole 1^{-+} scenario used to generate the pseudo-data, the closure refits confirm that the GlueX analysis chain recovers the generating solution, providing a validated baseline for forthcoming fits to experimental data. More generally, they illustrate how dispersive coupled-channel parameterizations, originally developed for hadroproduction, can be ported to photoproduction and used as building blocks for future global analyses across production mechanisms.

4.1 Outlook

The next step, already in progress, is to perform simultaneous fits of the coupled-channel amplitudes to the GlueX $\gamma p \to p\,\eta\pi^0$ and $\gamma p \to p\,\eta'\pi^0$ data, using the JPAC denominator $D^J(s)$ fixed to the COMPASS solution and varying only the complex photocouplings for each partial wave and channel. Such fits will test quantitatively whether the COMPASS-constrained coupled-channel amplitude, supplemented only by channel-dependent production strengths and phases, can describe the photoproduction data, and will provide a starting point for systematic studies in which the analytic parameterization and photoproduction kinematic factors are varied in a controlled way. In either case, combining a dispersive coupled-channel framework with high precision, polarized GlueX data is expected to sharpen the experimental constraints on gluonic excitations in the light-quark sector and help clarify the status of the $\pi_1(1600)$ as the leading hybrid candidate. More generally, coupled-channel analyses that combine GlueX photoproduction with complementary datasets will be essential to pin down the couplings of the lightest hybrid candidates.

Acknowledgments

This material is based upon work supported by the U.S. Department of Energy, Office of Science, Office of Workforce Development for Teachers and Scientists, Office of Science Graduate Student Research (SCGSR) program. The SCGSR program is administered by the Oak Ridge Institute for Science and Education (ORISE) for the DOE. ORISE is managed by ORAU under contract number DE-SC0014664. All opinions expressed in this paper are the author's and do not necessarily reflect the policies and views of DOE, ORAU, or ORISE. The work leading to this article was also partially supported by the U.S. Department of Energy, Office of Science, Office of Nuclear Physics under contract DOE Grant No. DE-FG02-87ER40315.

References

[1] J. Dudek, R. Edwards, P. Guo, and C. Thomas (Hadron Spectrum Collaboration), "Toward the excited isoscalar meson spectrum from lattice QCD," *Phys. Rev. D*, **88**, 094505 (2013), doi:10.1103/PhysRevD.88.094505.

[2] N. Isgur and J. Paton, "Flux-tube model for hadrons in QCD," *Phys. Rev. D*, **31**, 2910–2929 (1985), doi:10.1103/PhysRevD.31.2910.

[3] T. Barnes, F. E. Close, and E. S. Swanson, "Hybrid and conventional mesons in the flux tube model: Numerical studies and their phenomenological implications," *Phys. Rev. D*, **52**, 5242–5256 (1995), doi:10.1103/PhysRevD.52.5242.

[4] C. Adolph *et al.* (COMPASS Collaboration), "Odd and even partial waves of $\eta\pi^-$ and $\eta'\pi^-$ in $\pi^- p \to \eta^{(\prime)}\pi^- p$ at 191 GeV/c," *Phys. Lett. B*, **740**, 303–311 (2015), doi:10.1016/j.physletb.2014.11.058.

[5] A. Rodas *et al.* (Joint Physics Analysis Center Collaboration), "Determination of the Pole Position of the Lightest Hybrid Meson Candidate," *Phys. Rev. Lett.*, **122**, 042002 (2019), doi:10.1103/PhysRevLett.122.042002.

[6] S. Adhikari *et al.* (GlueX Collaboration), "The GlueX beamline and detector," *Nuclear Instruments and Methods in Physics Research Section A: Accelerators, Spectrometers, Detectors and Associated Equipment*, **987**, 164807 (2021), doi:10.1016/j.nima.2020.164807.

[7] F. Afzal *et al.* (GlueX Collaboration), "Upper limit on the photoproduction cross section of the spin-exotic $\pi_1(1600)$," *Phys. Rev. Lett.*, **133**, 261903 (2024), doi:10.1103/PhysRevLett.133.261903.

[8] A. Woss *et al.* (Hadron Spectrum Collaboration), "Decays of an exotic 1^{-+} hybrid meson resonance in QCD," *Phys. Rev. D*, **103**, 054502 (2021), doi:10.1103/PhysRevD.103.054502.

PoS(EPS-HEP2025)255